Surface States in the Photoionization of High-Quality CdSe Core/Shell Nanocrystals

Shu Li,* Michael L. Steigerwald, and Louis E. Brus

Chemistry Department, Columbia University, New York, New York 10027

Semiconductor nanocrystals are a model system for the size-tunability of electronic and optical properties, and they are components in electro- and quantum-optical devices.[1−3] Their high luminescence efficiency and photostability also make them valuable as sensitive luminescent probes in biological applications.[4] Photoluminescence intermittency ("blinking") is a nearly universal aspect of nanocrystal and nanowire luminescence, yet it is poorly understood. When it was first observed "blinking" was attributed to rare photoionization events; events in which optically excited electrons tunnel to a nearby trap state.[5] In that study it was observed that an insulating ZnS surface shell greatly decreased the blinking rate. Core/shell structures confine the exciton, typically increasing steady-state luminescence and decreasing carrier trapping on the nanocrystal surface.[6−8] A recent review concludes that blinking in TOPO-capped nanocrystals is indeed due to charge separation, with one carrier trapped in surface states that are intrinsic to the nanocrystal.[9] It is important to understand the relationship between charge separation in blinking, and in permanent photoionization, because both processes are critical to electrical transport properties in photovoltaic and electroluminescent devices, to optical gain in nanocrystal lasers, and to nanocrystal brightness for biological luminescence imaging.[10−12]

This proposed mechanism for blinking assumes that nanocrystals are not electrically doped (charged) as a direct result of the synthesis. In fact, solution-phase electrophoresis studies show nanocrystals often do have a few elementary charges.[13,14] To explore charging vis-à-vis blinking, we

ABSTRACT We use electric force microscopy (EFM) to study single nanocrystal photoionization in two classes of high-quality nanocrystals whose exciton luminescence quantum yields approach unity in solution. The CdSe/CdS/ZnS core/shell nanocrystals do not photoionize, while the CdSe/CdS nanocrystals do show substantial photoionization. This verifies the theoretical prediction that the ZnS shell confines the excited electron within the nanocrystal. Despite the high luminescence quantum yield, photoionization varies substantially among the CdSe/CdS nanocrystals. We have studied the nanocrystal photoionization with both UV (396 nm) and green (532 nm) light, and we have found that the magnitude of the charge due to photoionization per absorbed photon is greater for UV excitation than for green excitation. A fraction of the photoionization occurs directly *via* a "hot electron" process, using trap states that are either on the particle surface, within the ligand sphere, or within the silicon oxide layer. This must occur without relaxation to the thermalized, lowest-energy, emitting exciton. We discuss the occurrence of hot carrier processes that are common to photoionization, luminescence blinking, and the fast transient optical absorption that is associated with multiple exciton generation MEG studies.

KEYWORDS: nanocrystals · ionization · optical properties · hot electron · exciton · surface state

previously used EFM to directly observe the charge state of individual nanocrystals. In those studies the nanocrystals were immobilized under conditions similar to those used in luminescence studies. We found that dry nanocrystals were predominately neutral, and photoionization did occur for above-band gap irradiation at very low light intensities.[15,16] We extensively studied CdSe/CdS core shell nanocrystals on doped Si substrates that had thin (1−2 nm) surface oxides.[17−19] The doped silicon conductive substrate is not only required in EFM, but it also provides a nearby electron trap state of known characteristics. In the photoionizing event electrons move across both the TOPO capping layer and the 1−2 nm oxide and then into the silicon. We found a huge range of behavior in individual nanocrystals, and we suggested that this variability is related to nanocrystal structure defects. Some nanocrystals did not photoionize at
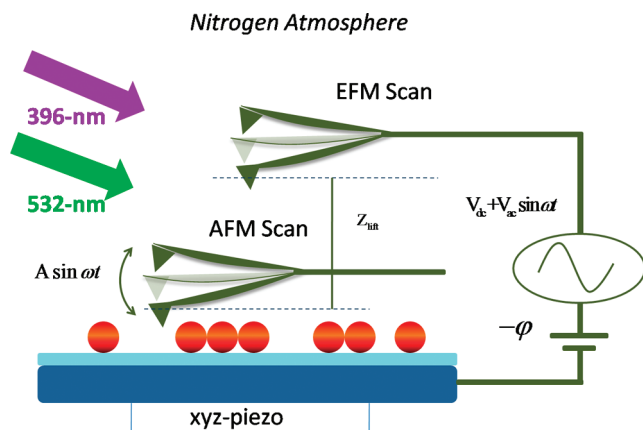
Nitrogen Atmosphere

Figure 1. EFM experimental setup.

all, while others showed multiple charges and/or different behavior for different irradiation wavelengths. In principle, just a single surface or interior defect is necessary to create a trapped carrier in a charge-separated dark state. In luminescence studies it is also often observed that while some nanocrystals luminesce strongly, others are completely dark; this is apparently due to a trap state that causes fast, nonradiative exciton recombination.

What is the intrinsic photoionization behavior of structurally perfect nanocrystals? It is, of course, difficult to assess structural perfection in nanocrystals, but as a practical working definition we suggest that a collection of perfect nanocrystals is one in which every nanocrystal shows luminescence. Here we extend our previous EFM study to such a collection of "perfect" nanocrystals. We study both CdSe/CdS core−shell nanocrystals (steady state luminescence QY = 0.93) and CdSe/CdS/ZnS nanocrystals (QY = 0.87). We also

study photoionization on Si substrates that have thick (300 nm) oxide layers. These experiments give new insight into the common occurrence of hot electron processes in long-distance photoionization, in luminescence blinking, and in fast transient optical absorption kinetics.

RESULTS

Our EFM/photoionization apparatus is illustrated in Figure 1. As previously described,[15,18] EFM is a variant of AFM in which a conductive probe is electrically connected to a conducting substrate. Nanocrystals are spun onto the substrate and studied under dry nitrogen at room temperature. Two passes are made for each scan line: the first records a regular tapping mode topograph of the sample; the second pass measures the shift of the resonance frequency of the tip when it is lifted a distance, z, above the substrate. In the second scan the tip is dithered mechanically at its natural frequency, and at the same time we apply a voltage, $V_{DC} + V_{AC} \sin(\omega t)$. (To simplify interpretation, we null out the contact potential difference φ between probe and substrate by setting $V_{DC} = -\varphi$.) As a consequence the ω force signal is due to the static electric field from the charges in the sample, and the 2ω force signal is due to the polarizability of the sample. We calculate the charge and dielectric constant of individual nanocrystals using a tip−sample capacitance analytical model.[20]

Samples were exposed to grazing angle, 396-nm light at ~15 mW/cm², or to 532-nm light (hereafter "UV" and "green", respectively) at ~50 mW/cm² for 3−6 h. During and after the irradiation we imaged the sample area continuously with the EFM in order to follow the evolution of the charge state of each particle.

After the laser was turned off, the samples were continuously imaged for 6−15 h.

In Figure 2 we show the simultaneously recorded topography and charge images for CdSe/CdS nanoparticles on n-type Si/14−Å SiO₂, with green and UV excitation in succession. Initially all nanoparticles are essentially neutral. Once the sample was exposed to cw green light many charged particles appeared. Steady state was reached after irradiation for ~180 min. After the laser was turned off, we observed no immediate charge decay. Subsequently in the dark most
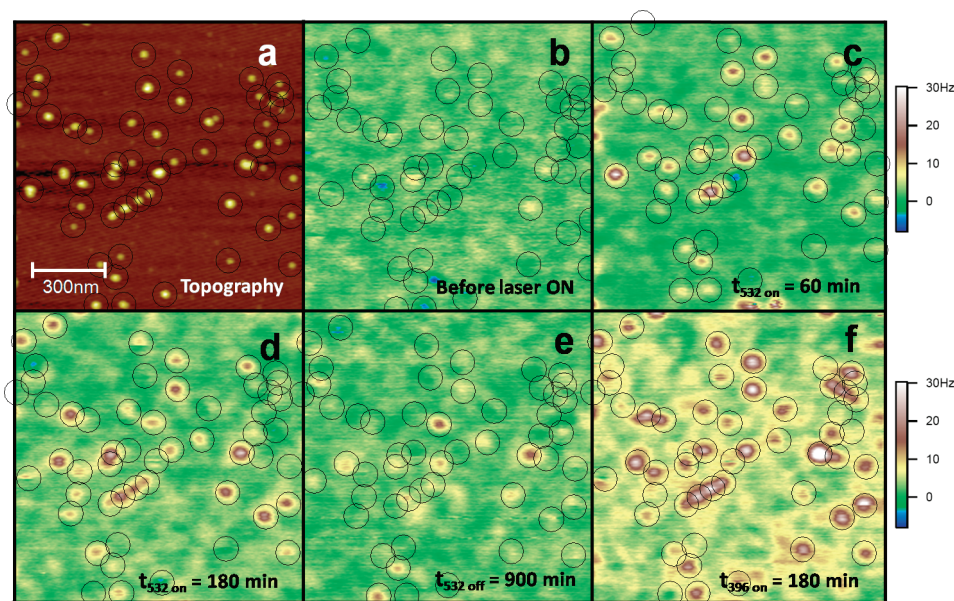

Figure 2. Topography (a) and charge (b−f) images of one area of CdSe/CdS nanocrystals on N-type Si with 14-Å SiO₂: (b) charge image before exposure; (c) charge image for green excitation after 60 min and (d) after 180 min; (e) charge image taken 15 h after the green laser is turned off; (d) charge image taken after UV exposure after 180 min.

nanocrystals return to the neutral state after roughly 15 h. If instead of turning off the laser, the green intensity is increased by a factor of 4 we observe essentially no change in the individual charge intensities (Figure S1 in Supporting Information). The charge intensity increases neither at higher laser intensity (over this limited range), nor for much longer exposures at the initial intensity. We exposed exactly the same field of nanocrystals to UV excitation (for similar times) only after the nanocrystals had decayed to their original neutral state overnight.

We calculated the charges on 83 single nanocrystals using the calibrated tip−substrate capacitance model. For each particle we measured the diameter and charge force gradient signal in the topology and EFM scans, respectively. A comparison between experimental and model-calculated force gradients is shown in Supporting Information, Figure S2. We show a sampling of our EFM results in Figure 3. Each panel describes the fate of a different individual particle. In each panel we show a topographic line scan (black, solid line) and three EFM scans: before irradiation (yellow squares), after green irradiation (green triangles), and after UV irradiation (blue diamonds). The topography profile indicates the size of the particle, and each EFM scan indicates the state of charge of the particle at the particular stage of the experiment. To estimate the charge magnitude we assumed that the charge was at the particle center in each case. These four particles demonstrate the general features of our observations for the 83 particles we studied. All of the particles were neutral before irradiation, and varying levels of charged developed after the two exposures. Particle "a" showed an effective charge of 1.1e after green irradiation and 2.4e after UV irradiation. Particle "b" did not ionize under green light, but was strongly charged after UV irradiation (2.2e). Particle "c" was equally charged by each color (1.6e under green and 1.7e under UV). Particle "d" did not ionize under green light and was comparatively modestly charged under UV (1.0e).

About 15% of the nanocrystals do not ionize under either green or UV irradiation; 40% of the nanocrystals do not ionize (defined as apparent charge magnitude less than 0.5) with green excitation. Of this group about two-thirds did ionize in the UV. In contrast 80% of the nanocrystals did ionize under UV irradiation; the average charge magnitude of this group is about 1.5. We summarize the ensemble in Figure 4. The histogram shows the number of particles in each of five charge ranges after each independent irradiation. In general,
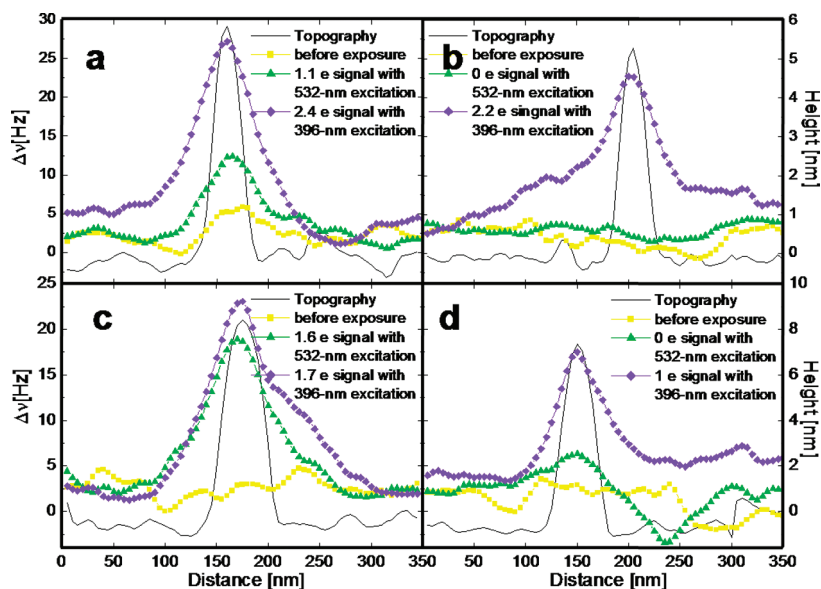

Figure 3. Topographic line scan of several charge profiles for the same CdSe/CdS particle on N-type Si with 14-Å SiO_2 and at several different times during photoexcitation experiments: uncharged, before exposure; the observed signals for each particles with 532-nm excitation showing charges of 1.1e (a), 0e (b), 1.6e (c), and 0e (d); and the observed signals for each particles with 396-nm excitation showing charges of 2.4e (a), 2.2e (b), 1.7e (c), and 1e (d).

nanocrystals that do charge develop a charge of larger magnitude under UV excitation than under green excitation.

In the experiment summarized in Figure 4 we used a Si substrate having a thin (1.4 nm) oxide layer. By way of contrast, we observed essentially no photoionization when the particles were deposited and irradiated on a substrate having a thick (300 nm) oxide layer (Supporting Information, Figure S3). We conclude, here as in our earlier work, that we are observing long-range photoionization—the charge is transferred from the nanocrystal all the way to the doped Si underneath the oxide. The 300 nm oxide is both too thick and too free of defects to allow carrier conduction to the Si.

The model-fitted charge magnitudes (Figure 4) do not show peaks at 1 and 2 positive charges; they are dis-
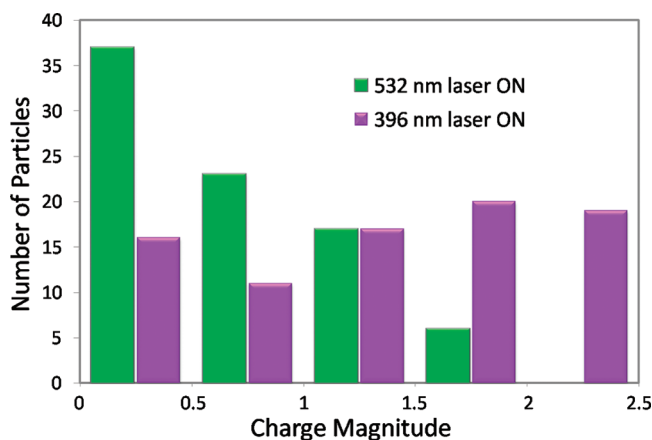

Figure 4. Histograms of charge counts observed during the course of photoexcitation experiments on N-type Si with 14-Å SiO_2 and with 532-nm and 396-nm excitations.
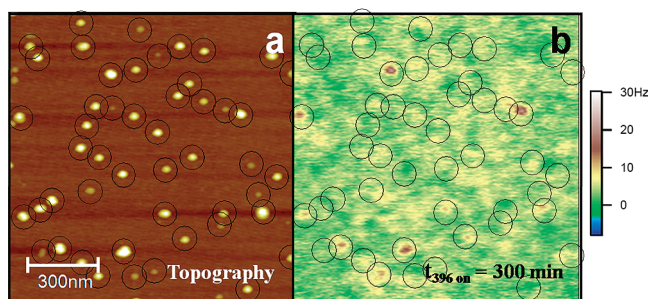
Figure 5. Topography (a) and charge image (b) of photoionization of CdSe/CdS/ZnS nanocrystals on N-type silicon with 14 Å SiO$_2$, exposed to 396-nm photoexcitation for 300 min.

tributed continuously. In our earlier work we observed poorly resolved peaks at integral charge. The model takes into account the measured diameters of individual nanocrystals, and thus accounts for the fact that the center of a larger nanocrystal is closer to the tip than the center of a smaller nanocrystal (for a given lift of the tip). The charge magnitude is sensitive to the position of the positive charge in the nanocrystal: a charge at the top gives a stronger signal (by almost a factor of 2) than does a charge at the bottom (*i.e.*, next to the oxide). It may be that some of the apparent variation in charge magnitude is due to the variability in the position for the charge. Our calibration model also assumes that the doped Si plane is an infinitely polarizable metal, forming a capacitor when combined with the metallic EFM tip. It may be that the conductivity of the doped Si and/or the thickness of the oxide are significantly heterogeneous across the surface; either would create variability in the calculated charge. It may also be that there are some photoionized electrons trapped under the nanocrystal at the doped Si oxide interface; these would have an additional weak charge signal of the opposite sign. Higher sensitivity and lower thermal noise could be achieved if this EFM study were repeated in high vacuum at low temperature.

Under similar experimental conditions the CdSe/CdS/ZnS nanocrystals show much less charging on the 1.4 nm oxide. Figure 5a,b shows the topography and charge images after prolonged (300 min) UV irradiation. Only 4 out of 50 particles ionize (each showing ∼1*e* positive charge). These two different core shell nanocrystals, CdSe/CdS and CdSe/CdS/ZnS, have the same surface ligands (TOPO/TOP), and similar luminescence quantum yields (0.93 and 0.87). Clearly the additional inorganic shell (ZnS) structure drastically reduces photoionization.

DISCUSSION

The behavior of these high-quality CdSe/CdS core shell nanocrystals is similar to the behavior we observed in earlier studies on nanocrystals of lower quality. Photoionization behavior is not uniform across the ensemble. About 40% of nanocrystals do not photoionize at all under green excitation; this is remarkable in

view of the fact that in solution essentially all of these nanocrystals luminescence (93% ensemble quantum yield). Of these 40% about two-thirds do photoionize under UV excitation. Thus there is a pathway for photoionization that is available *via* UV absorption but not *via* green absorption. Since the luminescing exciton is available by relaxation from either green or UV excitations, we conclude that for UV excitation there is some direct, "hot electron", photoionization that occurs without the system relaxing to the luminescing exciton state. It is apparent that, at both excitation wavelengths, there is a critical factor that varies from one nanocrystal to the next. It is likely that this is the availability and exact energy of a suitable trap state. This state may be on the nanocrystal surface, in its ligand shell, or in the nearby oxide. (We are not observing direct, very long-range electron tunneling from the core to the doped Si at either excitation wavelength. Such direct photoexcited electron transfer has been extensively characterized, mostly in a molecular and biological context.[21]) Thus, while we were expecting these structurally and chemically more perfect particles to behave qualitatively different than the more defective particles, they did not. This absence of improvement is itself striking.

Within the collection of nanocrystals that photoionize at both wavelengths, an individual nanocrystal, with a given oxide thickness underneath, typically shows a greater steady-state charge for UV excitation than green excitation. Green excitation typically produces a steady-state charge of 1 and UV excitation produces a charge of 2. The excitation rate (that is, the optical absorption cross section times the photon flux intensity) is about 3.6 times higher for the UV than the green. Yet, as described above, the magnitude of the charge does not increase when the green excitation intensity is increased by a factor of 4. Since in this latter situation the green excitation rate would then equal the UV excitation rate, the difference in excitation rates cannot account for the factor of 2 difference in ionization. Whatever the source, the net photoionization yield per absorbed photon is larger for UV excitation than for green excitation. We observed this result also in the detailed kinetic analysis of our earlier study. There we used a model that incorporated a much shorter lifetime for the UV (directly) excited-state than the (relaxed) green excited state; we found that the effective photoionization rate was 2−3 orders of magnitude higher for UV excitation.

We find that CdSe/CdS/ZnS nanocrystals show almost no photoionization in comparison to CdSe/CdS nanocrystals under identical conditions. Recall that a ZnS shell significantly slows down the rate of luminescence blinking and increases the ensemble exciton quantum yield.[5,22] Our result is consistent with electronic structure calculations in which a ZnS shell more

completely confines the electron wave function to the inner core in comparison with a CdS shell.[23,24]

The light intensities we use are approximately 10^3 lower than those typically used in luminescence studies. In luminescence blinking the off times are independent of excitation intensity. Our calculated absolute quantum yield for photoionization is low ($\sim 10^{-6}$). In hexane solution the luminescence excitation spectrum closely tracks the absorption spectrum (Supporting Information, Figure S4), thus the predominant fate of the initially excited high-energy "hot electron" state is relaxation to the luminescing, thermalized exciton.

Both photoionization and luminescence blinking involve surface states that imply charge-separation, although the time scales in the two processes differ significantly: the photoionization events we observe occur on far longer time scales than "off" events in luminescence blinking studies. In luminescence blinking, the "off" state durations range from milliseconds to a few seconds, and the distribution is independent of excitation intensity. The electron or hole, which had been trapped on the surface, returns to the core on these time scales. Our EFM study only records "long-range" photoionization events, and these last for many minutes or hours. In blinking studies if an "off" period lasted this long, one would claim that the nanocrystal had permanently photodarkened. In our EFM studies electrons transfer ultimately to the doped Si from the nanocrystal core, across the organic ligands and the oxide; luminescence blinking is thought to involve nanocrystal surface states,[9] and therefore the relaxation to the "on" state should be much faster.

Recent experiments have shown that the blinking kinetics in CdSe/ZnS nanocrystals and in CdSe nanorods also depends upon the excitation wavelength.[25,26] A 240 meV threshold (above the thermalized exciton) separating two behavior regimes was discovered. For higher photon energy excitation, "off" periods were longer than for lower energy excitation. Knappenberger *et al.* concluded that different, more spatially distant trap states, taking longer to tunnel back to the core, are populated at higher energy. These authors also used an ionic liquid to increase the external dielectric coefficient around the nanocrystal. For high-energy excitation, long "off" time periods (approaching 10 s) significantly increased in the presence of the high external dielectric constant. This suggests dielectric stabilization, and thus slower return, of photoexcited charge outside the core near the liquid. This behavior was not observed for low-energy excitation. In an earlier experiment "off" times also lengthened in hosts with larger dielectric constant.[27] The energy of a surface trapped charge should be lowered (relative to the core) in a higher dielectric constant host.

The study by Knappenberger *et al.* shows that a component of the trapping leading to "off" periods occurs directly from the initial high-energy photoexcited state, and does not proceed through the relaxed thermalized exciton. This is the same conclusion we reach here in EFM studies of long-lived photoionization events.

In various nanocrystal systems, fast transient optical absorption kinetics has been intensively studied, for low intensity excitation at photon energies far above the size-dependent nanocrystal band gap.[28−30] These studies explore multiple exciton generation (MEG). High photon energy excitation shows a lowest exciton bleach picosecond optical transient (not seen for low energy excitation) on top of the normal long-lived nanosecond bleach transient of thermalized excitons in neutral nanocrytals. The data vary with the choice of surface ligand choice and from sample to sample. Transients increase with exposure to high photon energy excitation in unstirred samples. As recently suggested by Klimov, these data likely (in part) represent prior "photoionization".[29] We suggest that high photon-energy excitation creates an inhomogeneous sample composed of both neutral and long-lived charge-separated nanocrystals. It is likely that in the latter the hole is trapped on the surface and the electron is in an interior core 1S state. Such "photoionized" nanocrystals are not created by low photon energy, direct excitation of the emitting exciton. This subject remains unsettled.

All three physical processes (photoionization, luminescence blinking, and transient optical absorption) seem to involve enhanced interaction with surface states *via* high photon-energy excitation. Why are surface states present in nanocrystals with high luminescence quantum yields? It is known that surface structural relaxation and ligand passivation do not eliminate surface states. Rather, relaxation and passivation shift surface state energies away from the band gap center toward the electron and hole quantum-confined core energies. Electronic structure calculations show a wide range of surface-localized electron states that are in resonance with core electron states in typical CdSe nanocrystals.[31] In our particles, which show strong exciton emission, passivation has likely shifted the majority of surface states to energies higher than the relaxed, luminescing exciton. Even in nanocrystals that show strong exciton emission without lower energy trap emission, the relaxed, lowest-lying core exciton remains weakly coupled to unpassivated surface states. This weak coupling is shown by the presence of the luminescence zero phonon line at 4 K in the spectrum,[32] and by the multiexponential nature of exciton time decay at room temperature.[33] At higher energies above the emitting exciton, the interaction between core states and surface states is likely stronger, leading to the type of hot carrier effects discussed here. It is an important experimental goal to obtain the low temperature optical absorption or luminescence excitation spectrum of a single nanocrystal, to search for possible

spectral evidence of stronger coupling between core states and surface states.

CONCLUSION

We have expanded on a previous EFM-based study of core/shell semiconductor nanocrystals by examining materials of exceptionally high optical quality.

We have observed that even though these nanocrystals photoluminesce with very high quantum yields, their tendency to photoionize varies significantly across the ensemble. By contrasting the behavior of these nanocrystals under short- *versus* long-wavelength irradiation, we conclude that the photoionization occurs in part *via* hot carriers that use as yet ill-defined trap states on the ionization pathway.

METHODS

CdSe/CdS TOPO/TOP capped nanocrystals (7−8 nm, 1.8 μM in hexane) and CdSe/CdS/ZnS TOPO/TOP capped nanocrystals (8−9 nm, 2.5 μM in hexane) were generous gifts from Invitrogen. These solutions were stored in hexane under nitrogen in the dark. Before we used these solutions we diluted each by a factor of 20 with fresh hexane. The diluted samples were spun onto N-type (Sb-doped, 0.008−0.03 Ω cm) silicon substrates that had a surface layer of 1.4 nm thermal oxide (IBM Research). The substrates were cleaned with ethanol and hexane prior to particle deposition. We minimized the exposure of the nanoclusters to air (<10 min, during sample preparation) to prevent photooxidation. We refer to these two different nanocrystal samples as "CdS shell" and "ZnS shell", respectively. We prepared similar samples on P-type silicon substrates having a 300-nm oxide layer.

EFM experiments were performed in a glovebox under nitrogen atmosphere at room temperature ($P(O_2) < 3$ ppm, $P(H_2O) < 1$ ppm) using a Digital Instruments Multimode AFM with an extender module. Calibrated Cr/Pt coated EFM tips (BS-ElectriMulti75) from Nanoscience Instruments Inc. were used, with resonance frequencies around 75 kHz and spring constants measured to be around 1.7 N/m. The typical topography feedback set-point was 0.37 V, and the photodiode sensitivity was 13 nm/V.

Sample were exposed to grazing angle, 396-nm light from a diode laser (Coherent, RA 0222-583-00) at ∼15 mW/cm², or to 532-nm light from a diode laser (Information Unlimited, model LAGR50M) at ∼50 mW/cm², while being continuously imaged for 3−6 h. After the laser was turned off, the samples were continuously imaged for 6−15 h to observe the electrical reneutralization. CdSe/CdS nanoparticles on the N-Si/14 Å SiO₂ substrate were exposed to 396-nm and 532-nm laser in succession. Image data were analyzed using Igor 4.0 and all mathematical modeling was done using Mathematica 4.1.

Supporting Information Available: Figures S1−S4. This material is available free of charge *via* the Internet at http://pubs.acs.org.

REFERENCES AND NOTES

1. Klimov, V. I.; Mikhailovsky, A. A.; Xu, S.; Malko, A.; Hollingsworth, J. A.; Leatherdale, C. A.; Eisler, H. J.; Bawendiz, M. G. Optical Gain and Stimulated Emission in Nanocrystal Quantum Dots. *Science* **2000**, *290*, 314–317.

2. Wang, C.; Shim, M.; Guyot-Sionnest, P. Electrochromic Nanocrystal Quantum Dots. *Science* **2001**, *291*, 2390–2392.

3. Huynh, W. U.; Dittmer, J. J.; Alivisatos, A. P. Hybrid Nanorod-Polymer Solar Cells. *Science* **2002**, *295*, 2425–2427.

4. Dubertret, B.; Skourides, P.; Norris, D. J.; Noireaux, V.; Brivanlou, A. H.; Libchaber, A. *In Vivo* Imaging of Quantum Dots Encapsulated in Phospholipid Micelles. *Science* **2002**, *298*, 1759–1762.

5. Nirmal, M.; Dabbousi, B. O.; Bawendi, M. G.; Macklin, J. J.; Trautman, J. K.; Harris, T. D.; Brus, L. E. Fluorescence Intermittency in Single Cadmium Selenide Nanocrystals. *Nature (London)* **1996**, *383*, 802–805.

6. Spanhel, L.; Haase, L.; Weller, H.; Henglein, A. Photochemistry of Colloidal Semiconductors 20: Surface Modification and Stability of Strong Luminescing CdS Particles. *J. Am. Chem. Soc.* **1987**, *109*, 5649–5655.

7. Kortan, R.; Hull, R.; Opilia, R.; Bawendi, M.; Steigerwald, M.; Carroll, P.; Brus, L. Nucleation and Growth of Cadmium Selenide on Zinc Sulfide Quantum Crystallites, and *vice versa*, in Inverse Micelle Media. *J. Am. Chem. Soc.* **1990**, *112*, 1327–1332.

8. Hines, M.; Guyot-Sionnest, P. Synthesis and Characterization of Strongly Luminescing Zn Capped CdSe Nanocrystals. *J. Phys. Chem.* **1996**, *100*, 468–473.

9. Gomez, D; Califano, M.; Mulvaney, P. Optical Properties of Single Semiconductor Nanocrystals. *Phys. Chem. Chem. Phys.* **2006**, *8*, 4989–5011.

10. Malko, A. V.; Mikhailovsky, A. A.; Petruska, M. A.; Hollingsworth, J. A.; Htoon, H.; Bawendi, M. G.; Klimov, V. I. From Amplified Spontaneous Emission to Microring Lasing Using Nanocrystal Quantum Dot Solids. *Appl. Phys. Lett.* **2002**, *81*, 1303–1305.

11. Michalet, X.; Pinaud, F.; Lacoste, T. D.; Dahan, M.; Bruchez, M. P.; Alivisatos, A. P.; Weiss, S. Properties of Fluorescent Semiconductor Nanocrystals and their Application to Biological Labeling. *Single Molecules* **2001**, *2*, 261–276.

12. Mikhailovsky, A. A.; Malko, A. V.; Hollingsworth, J. A.; Bawendi, M. G.; Klimov, V. I. Multiparticle Interactions and Stimulated Emission in Chemically Synthesized Quantum Dots. *Appl. Phys. Lett.* **2002**, *80*, 2380–2382.

13. Islam, M. A.; Herman, I. P. Electrodeposition of Patterned CdSe Nanocrystal Films Using Thermally Charged Nanocrystals. *Appl. Phys. Lett.* **2002**, *80*, 3823–3825.

14. Jia, S.; Banerjee, S.; Herman, I. P. Mechanism of the Electrophoretic Deposition of CdSe Nanocrystal Films: Influence of the Nanocrystal Surface and Charge. *J. Phys. Chem. C* **2008**, *112*, 162–171.

15. Krauss, T. D.; Brus, L. E. Charge, Polarizability and Photoionization of Single Semiconductor Nanocrystals. *Phys. Rev. Lett.* **1999**, *83*, 4840–4843.

16. Krauss, T. D.; O'Brien, S.; Brus, L. E. Charge and Photoionization Properties of Single Semiconductor Nanocrystals. *J. Phys. Chem. B* **2001**, *105*, 1725–1733.

17. Ben-Porat, C. H.; Cherniavskaya, O.; Brus, L.; Cho, K.-S.; Murray, C. B. Electric Fields on Oxidized Silicon Surfaces: Static Polarization of PbSe Nanocrystals. *J. Phys. Chem. A* **2004**, *108*, 7814–7819.

18. Cherniavskaya, O.; Chen, L.; Islam, M. A.; Brus, L. Photoionization of Individual CdSe/CdS Core/Shell Nanocrystals on Silicon with 2-nm Oxide Depends on Surface Band Bending. *Nano Lett.* **2003**, *3*, 497–501.

19. Cherniavskaya, O.; Chen, L.; Brus, L. Imaging the Photoionization of Individual CdSe/CdS Core−Shell Nanocrystals on n- and p-Tpye Silica on Substrates with Thin Oxides. *J. Phys. Chem. B* **2004**, *108*, 4946–4961.

20. Cherniavskaya, O.; Chen, L.; Weng, V.; Yuditsky, L.; Brus, L. E. Quantitative Noncontact Electrostatic Force Imaging of Nanocrystal Polarizability. *J. Phys. Chem. B* **2003**, *107*, 1525–1531.

21. Gray, H.; Winkler, J. Long Range Electron Transfer. *Proc. Nat. Acad. Sci. U.S.A.* **2005**, *102*, 2534–2537.

22. Morelli, G.; Anni, M.; Cozzoli, P.; Manna, L.; Cingolani, R.; DeGiorgi, M. The Role of Intrinsic and Surface States in the Emission Properties of Colloidal CdSe and CdSe/ZnS Quantum Dots. *Nanoscale Res. Lett.* **2007**, *2*, 512–514.

23. Peng, X.; Schlamp, M. C.; Kadavanich, A. V.; Alivisatos, A. P. Epitaxial Growth of Highly Luminescent CdSe/CdS Core/Shell Nanocrystals with Photostability and Electronic Accessibility. *J. Am. Chem. Soc.* **1997**, *119*, 7019–7029.

24. Dabbousi, B. O.; Rodriguez-Viejo, J.; Mikulec, F. V.; Heine, J. R.; Mattoussi, H.; Ober, R.; Jensen, K. F.; Bawendi, M. G. (CdSe)ZnS Core−Shell Quantum Dots: Synthesis and Characterization of a Size Series of Highly Luminescent Nanocrystallites. *J. Phys. Chem. B* **1997**, *101*, 9463–9475.

25. Knappenberger, K., Jr.; Wong, D.; Romanyuk, Y.; Leone, S. Excitation Wavelength Dependence of Fluorescence Intermittency in CdSe/ZnS Core/Shell Quantum Dots. *Nano Lett.* **2007**, *7*, 3869–3874.

26. Knappenberger, K., Jr.; Wong, D.; Xu, W.; Schwartzberg, A.; Wolcott, A.; Zhang, J.; Leone, S. Excitation-Wavelength Dependence of Fluorescence Intermittency in CdSe Nanorods. *ACS Nano* **2008**, *2*, 2143–2153.

27. Issac, A.; von Borezyskowski, C.; Cichos, F. Correlation between Photoluminescence Intermittency of CdSe Quantum Dots and Self-Trapped States in Dielectric Media. *Phys. Rev. B* **2005**, *71*, 161302.

28. Klimov, V. Spectral and Dynamical Properties of Multiexcitons in Semiconductor Nanocrystals. *Annu. Rev. Phys. Chem.* **2007**, *58*, 635–637.

29. Schaller, R.; Agranovich, V.; Klimov, V. High Efficiency Carrier Multiplication through Direct Photogeneration of Multi-Excitons *via* Virtual Single Exciton States. *Nat. Phys.* **2005**, *1*, 189–141.

30. Ellingson, R.; Beard, M.; Johnson, J.; Yu, P.; Micic, O.; Nozik, A.; Shabaev, A.; Efros, A. Highly Efficient Multiple Exciton Generation in Colloidal PbSe and PbS Quantum Dots. *Nano Lett.* **2005**, *5*, 865–871.

31. Bryant, G.; Jaskolski, W. Surface Effects on Capped and Uncapped Nanocrystals. *J. Phys. Chem. B* **2005**, *109*, 19650–19656.

32. Califano, M.; Franceschetti, A.; Zunger, A. Temperature Dependence of Excitonic Radiative Decay in CdSe Quantum Dots: The Role of Surface Hole Traps. *Nano Lett.* **2005**, *5*, 2360–2364.

33. Jones, M.; Lo, S.; Scoles, G. Quantitative Modeling of the Role of Surface Traps in CdSe/CdS/ZnS Nanocrystal Photoluminescence Decay Dynamics. *Proc. Natl. Acad. Sci. U.S.A.* **2009**, *106*, 3011−3016.